Chin. Geogra. Sci. 2009 19(3) 283–290
DOI: 10.1007/s11769-009-0283-x
www.springerlink.com

# Improvement of Urban Impervious Surface Estimation in Shanghai Using Landsat7 ETM+ Data

YUE Wenze
(*Department of Land Management, Zhejiang University, Hangzhou 310029, China*)

**Abstract:** This paper explores the potential to improve the impervious surface estimation accuracy using a multi-stage approach on the basis of vegetation-impervious surface-soil (V-I-S) model. In the first stage of Spectral Mixture Analysis (SMA) process, pixel purity index, a quantitative index for defining endmember quality, and a 3-dimensional endmember selection method were applied to refining endmembers. In the second stage, instead of obtaining impervious surface fraction by adding high and low albedo fractions directly, a linear regression model was built between impervious surface and high/low albedo using a random sampling method. The urban impervious surface distribution in the urban central area of Shanghai was predicted by the linear regression model. Estimation accuracy of spectral mixture analysis and impervious surface fraction were assessed using root mean square (RMS) and color aerial photography respectively. In comparison with three different research methods, this improved estimation method has a higher overall accuracy than traditional Linear Spectral Mixture Analysis (LSMA) method and the normalized SMA model both in root mean square error (RMSE) and standard error (SE). However, the model has a tendency to overestimate the impervious surface distribution.

**Keywords:** vegetation-impervious surface-soil model; spectral mixture analysis; impervious surface; Shanghai

## 1 Introduction

The status and trend of urban land use and land cover significantly impact the quality of human being's life and urban ecosystems. Accurate, up-to-date and spatially explicit data on urban land use and land cover are required to support urban land management decision-making, ecosystem monitoring and urban planning. Ridd (1995) proposed the vegetation-impervious surface-soil (V-I-S) model for parameterizing biophysical composition of urban environments. In this model, urban land use and land cover classes can be modeled by the fraction of vegetation, impervious surface, and soil (Wu and Murray, 2003). The V-I-S model, especially impervious surface fraction might be a basis for a better understanding of urban environments, including both physical geography (urban heat islands, runoff modeling and urban change detection) and human geography (population density estimation and quality of life assessment) (Ridd, 1995).

However, due to the difficulties in the impervious surface estimation, the V-I-S model is only considered conceptually with limited applications. Although different approaches have been developed (Deguchi and Sugio, 1994; Ji and Jesen, 1999; Slonecker et al., 2001; Brabec et al., 2002; Wu, 2004), the impervious surface extraction is still a challenge because of the complexity of urban landscape and limitation of remotely sensed data in spectral and spatial resolutions (Lu and Weng, 2005). Recently, the V-I-S conceptual model has been successfully applied by using the technique of spectral mixture analysis (SMA). Small (2001; 2004) estimated urban vegetation distribution using a three-endmember linear mixture model, and also expressed difficulties associated with impervious surface estimation. Wu and Murray (2003) introduced a method for estimating impervious surface distribution using linear spectral mixture analysis and first suggested a linear relationship formula. Though the model was not really fulfilled in practice instead of a method by adding high/low albedo

Received date: 2008-12-22; accepted date: 2009-05-04
Foundation item: Under the auspices of National Natural Science Foundation of China (No. 40701177)
Corresponding author: YUE Wenze. E-mail: wzyue@zju.edu.cn

fractions directly, it is significant to understand the composition of impervious surface from the view of remote sensing spectrum. Yue and Wu (2007) made a SMA application, in which they derived impervious surface fraction by adding high/low albedo fractions directly using the method of Wu and Murray (2003). Wu (2004), Weng and Lu (2008) estimated urban impervious surface by a new normalized spectral mixture analysis method, which at first assumes that spectrum shape is similar besides brightness difference between high/low albedo endmember, then derives impervious surface faction from the SMA model directly by considering impervious surface as one endmember. Although the estimation accuracy had been improved, according to on-spot spectrum measurement in Chinese urban area, the spectrum divergence among urban impervious surface types is so dramatic. The difference puts up not only on spectrum brightness, but also on spectrum pattern. It was very difficult to normalize impervious surface as one endmember (Yue et al., 2006).

In general SMA procedure, selecting suitable endmembers is very important to obtain high quality fraction images and the key factor to determine the overall accuracy (Weng and Lu, 2008). However existing studies seldom adopted a quantitative criterion to gauge the quality of selected endmembers, thus it was very hard to duplicate the estimate results (Wu and Murray, 2003; Wu, 2004; Lu and Weng, 2005; 2006). Additionally, in existing researches, all endmember selection is from two-dimensional feature space after minimum noise fraction (MNF) transformation, which would facilitate the selection while be opt to miss information. In this paper, improvements were introduced to estimate urban impervious surface fraction. Firstly, a quantitative index of endmember quality, PPI (Pixel Purity Index) and an endmember selection method in 3-dimensional pixel feature space were applied to assisting the endmember selection. Secondly, it is the first time to estimate the impervious surface faction by a quantitative regression model between impervious surface faction and high and low albedo fractions.

## 2 Data and Methods

### 2.1 Study area

Shanghai is located on the east coast of China (Fig. 1). For more than one and half centuries since about 1850, Shanghai has been China's biggest economic center. Under the period of planned economy (1949–1978) in China, Shanghai became an industrial production center (Cai and Victor, 2003). Its urban development has progressed at an unprecedented pace since the implementation of the economic reforms after 1978 (Xu et al., 2004). According to the Fifth Population Census in 2000, there were more than 9,150,000 people in an area of 660km$^2$ inside Out Ring Road, and the population density got to 14,000 person/km$^2$. So, the building density and road density were very higher. In order to describe the composition of urbanized area, the urban central area inside Out Ring Road was put on more consideration in this study (Fig. 1).

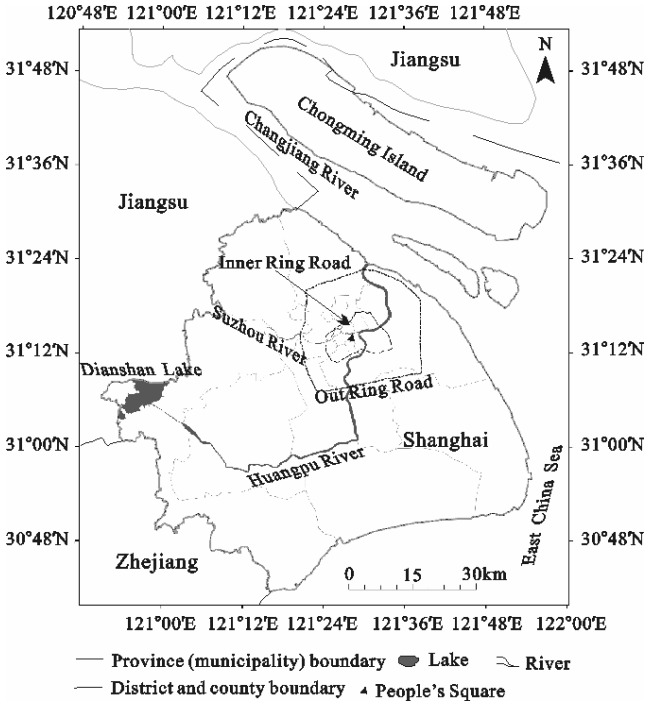


Fig. 1 Location of study area

### 2.2 Data set

The Landsat 7 ETM+ images (path 118/row 38; path 118/row 39) received on June 14, 2000 were served as the primary data sources. The data were acquired under a very clear atmospheric condition by National Remote Sensing Center of China (NRSCC), and the radiometric and geometrical distortions of the images have been improved to a 1G level before delivery. After a radiometric enhancement, the image was then further rectified to a Shanghai coordinate system (a modified Transverse Mercator coordinate system), and was re-

sampled using the nearest neighbor algorithm with a pixel size of 30m×30m. The resultant root mean square error (RMSE) was found to be less than 0.5 pixels. No atmospheric calibration was conducted for the ETM+ image, because previous research had demonstrated that atmospheric calibration did not have an effect on fraction images if image endmembers were used (Lu and Weng, 2006; Small, 2004). The aerial photographs for entire Shanghai urban area were acquired in August 2000. It had a spatial resolution of 1m, and was reprojected to ETM+ image's coordinate system after being merged. Aerial photograph was used for deriving water surface distribution and validation of impervious surface estimation. The boundary of water surface distribution was derived by manual digitizing way. Then the vector map was used to mask the water distribution of Landsat7 ETM+ image.

### 2.3 Methods

#### *2.3.1 Linear Spectral Mixture Analysis*

Linear Spectral Mixture Analysis (LSMA) is a method physically based on image processing, which assumes that spectrum measured by a sensor is a linear combination of the spectra of all components within the pixel. It is the simplest condition of SMA. It can be expressed as (Small, 2004):

$$R_i = \sum_{k=1}^{n} f_k R_{ik} + ER_i \quad (1)$$

where $R_i$ is the spectral reflectance of band $i$ which contains one or more endmembers, $i$=1, 2, 3…$m$; $f_k$ is the proportion of endmember $k$ within a pixel, $k$=1, 2, 3…$n$; $R_{ik}$ is the known spectral reflectance of endmember $k$ within the pixel on band $i$; and $ER_i$ is the error for band $i$. Root mean square (RMS) was used to measure the accuracy of solution:

$$RMS = \sqrt{(\sum_{i=1}^{m} ER_i^2)/m} \quad (2)$$

A constrained inverse least squares deconvolution model was used in this research, assuming that the following two conditions are satisfied simultaneously:

$$\sum_{k=1}^{n} f_k = 1 \quad \text{and} \quad 0 \le f_k \le 1$$

This will restrict each endmember fraction between 0 and 1, and all the summation is equal to 1, which can avoid any fraction larger than 1 or smaller than 0.

The minimum noise fraction (MNF) transformation can reduce the correlation between bands and concentrate most information on the first several components, which can improve the accuracy of LSMA as a result (Lu and Weng, 2005). Unlike principal component transformation, the MNF transformation orders the components according to the ratio of signal to noise (Green et al., 1988).

In the LSMA process, endmember selection is a key step. An optimal approach for selecting endmembers is using laboratory-based measurements of endmember's spectra, defined as "reference endmember". Although substantial problems exist in correcting atmospheric conditions in satellite sensor data, they are solved by considering the mixed spectra as a linear combination of endmembers derived from an image (image endmember) (Lu et al., 2003). In practice, image endmember selection methods are frequently used, because endmenbers can be easily obtained and they represent the spectra measure at the same scale as the image data (Lu and Weng, 2006). Image endmembers could be derived from the extremes of the image feature space, assuming that they represent the purest pixels in the images (Mustard and Sunshine, 1999). In this paper, image endmembers were also seclected from the feature spaces formed by MNF components.

#### *2.3.2 First stage improvement*

In order to improve the quality of endmember, two measures were adopted to aid the selection process. In the first step, a Pixel Pure Index (PPI) of ENVI was introduced to constrict the selection range of very pure pixels. In the study area, the number of pixels is 1,665,292, after PPI iteration computation, the remaining pure pixel is 71,046 which accounts for 4.26% of total pixels. At the same time each selected pixel had a measurable index to describe the pure degree. A mask image gained from PPI result was used to filter pure pixels. Then pure pixels which represented endmembers could be selected. Through PPI, the range of selection was reduced by near 95%. In the next step, we used a 3-dimensional endmember selection tool with a user-friendly graphical interface in place of the unapproachable GUI provided by ENVI (Fig. 2). In the tool, the coordinate axis could be circumrotated and tilted, and polyhedron by pixels formation and its projections on three sides could be observed at the same time. A linkage was built between the pixels in the 3D feature space and PPI result so that the spatial position and purity can be easily

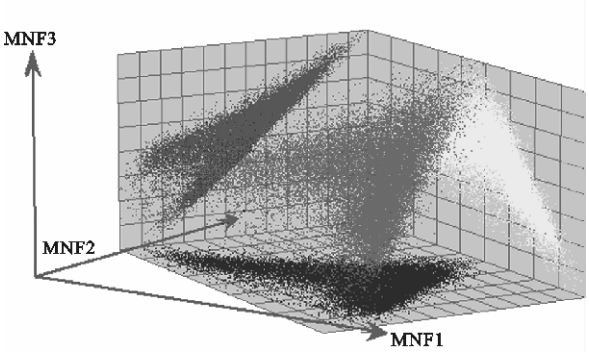


MNF1–3 represent the first three components of minimum noise fraction transformation respectively

Fig. 2 Pixel scatter plot in 3D space

checked by interactive comparison.

### *2.3.3 Second stage improvement*

According to Ridd's V-I-S model, the high/low albedo endmembers could not be directly interpreted as impervious surface. Thus, finding a relationship between the high and low albedo endmembers and impervious surface was important (Ridd, 1995). Wu and Murray (2003) considered that most impervious surfaces might be represented by low and high albedo endmembers as follows.

$$R_{\text{imp,b}}=f_{\text{low}}R_{\text{low,b}}+f_{\text{high}}R_{\text{high,b}}+e_{\text{b}} \quad (3)$$

where $R_{\text{imp,b}}$ is the reflectance spectra of impervious surfaces for band b, and $f_{\text{low}}$ and $f_{\text{high}}$ are the fraction of low albedo and high albedo, respectively. $R_{\text{low,b}}$ and $R_{\text{high,b}}$ are the reflectance spectra of low and high albedo for band b, and $e_{\text{b}}$ is the unmodeled residual. Associated with determining $R_{\text{imp,b}}$ is the requirement of $f_{\text{low}}+f_{\text{high}}\leq 1$, $f_{\text{low}}\geq 0$ and $f_{\text{high}}\geq 0$.

But in the process of estimation, Wu and Murray (2003) did not use this model instead of adding the fractions of high/low albedo endmenbers directly. According to the principle of LSMA, there should be a linear relationship between high and low albedo endmembers. But we are not well known the quantitative relationship between impervious surface fraction and high/low albedo fractions. In this paper, we also assumed that a pure impervious surface land cover type might be modeled by high/low albedo types excluding water surface. The simplest relationship between impervious surface and high, low albedo endmembers is linear, and then we got Equation (4).

$$F_{\text{imp}}=af_{\text{low}}+bf_{\text{high}}+c \quad (4)$$

where $F_{\text{imp}}$ is the fraction of impervious surfaces for each pixel; $f_{\text{low}}$ and $f_{\text{high}}$ are the fractions of low albedo and high albedo, respectively; $a$ and $b$ are the function coefficients between low and high albedo endmembers and impervious surface; and $c$ is constant.

Then in order to estimate the parameters in Equation (4), a regression model was introduced through random sampling. At first, we generated 239 square window samples randomly with a size of 150m×150m in aerial photograph (Fig. 3) and then, we digitalized the impervious surface manually in the 239 windows and obtained the 'really' percent of impervious surface for each sample. Then, values of high and low albedo fraction were derived from the modeled unmixing results by a GIS (Geographic Information System) zonal statistics method. And 94 samples among all samples were put into model and the rest 145 samples would be used to assess the accuracy of impervious surfaces estimation.

## 3 Results

### 3.1 Fraction image calculation

After the first stage improvement, three endmembers of vegetation (grass and trees), high-albedo (metal material,

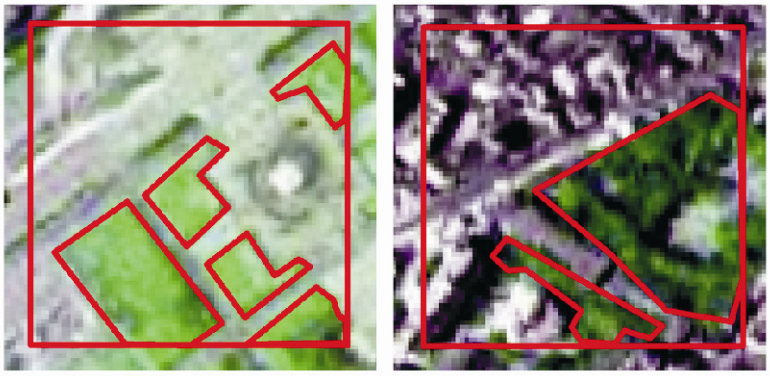

Fig. 3 Sample demonstration in aerial photograph

new concrete surface, sand and some compound material), low-albedo (old concrete surface, cyan tile and asphalt) were identified and selected from feature spaces. The spectra values of endmembers were shown in Fig. 4.

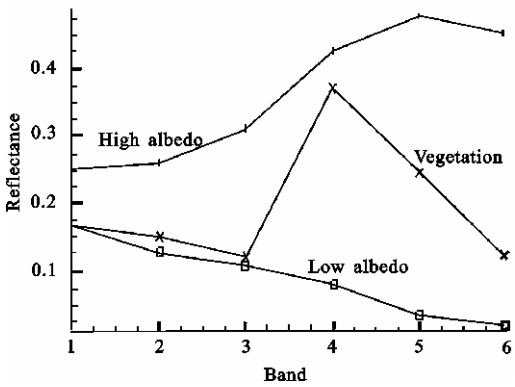


Fig. 4 Reflectance of three endmembers at six bands

The endmember fraction images (Fig. 5) were calculated by solving a fully constrained three-endmember linear mixing model using the Landsat7 ETM+ data. The vegetation fraction image correlated with known green areas within the original image. That is, the vegetation fraction changed from near zero in urban center to high value in the area near Out Ring Road. Most low albedo fraction was above 50% inside Inner Ring Road, and decreased fast in non-built-up area. High albedo fraction was mainly located in urban sprawling area.

The RMS maximum of LSMA was 0.0867, and 98.5% of RMS values were smaller than 0.02. The RMS values of urban central area were higher than those of outer area, and those of old city area were also higher than those of newly-built urban area. Comparatively, mixed pixels were inclined to have larger RMS than pure pixels. The more

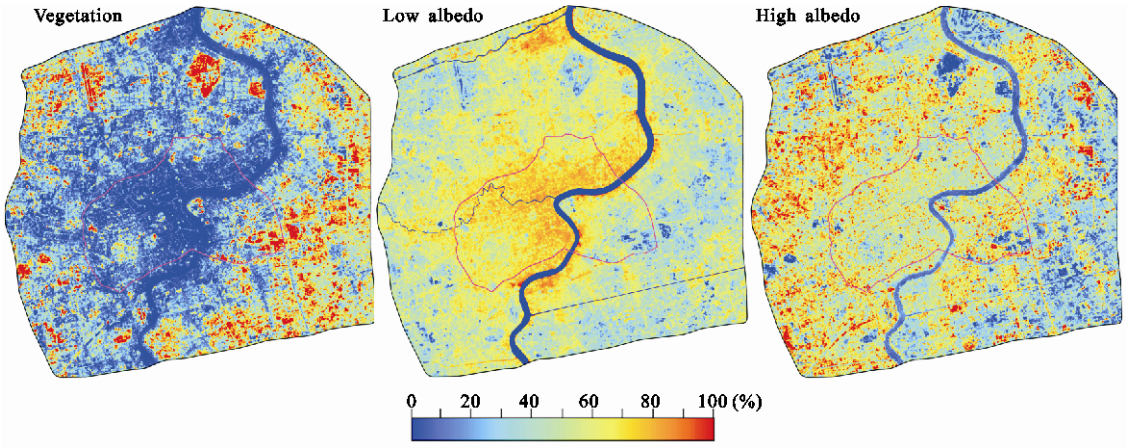


Fig. 5 Three endmember fraction images inside Out Ring Road after unmixing

complicated the inside mixed pixel was, the larger the RMS would be, which suggests that there may be another spectral endmember, for example shade.

### 3.2 Impervious surface estimation

In the second improvement process, 94 random samples were selected to estimate the parameters of above-mentioned model by a linear regression method of SPSS. The results of parameter estimation appear as Equation (5). The estimated model and parameters had passed the *t* test, *F* test and Durbin-Watson test respectively.

$$R_{\text{imp}} = 1.283R_{\text{low}} + 0.890R_{\text{high}} - 0.188 \quad (5)$$

(Std. error: 0.077, 0.112, 0.055)

($R^2$=0.796 Adjusted $R^2$=0.792 $N$=94)

Vegetation shade can be identified through detailed studies of urban vegetation canopy structure (Gilabert et al., 2000). In this research area, most vegetation surface was artificial lawn. So the effect of vegetation shade was ignored. Water surfaces were masked by digitized water cover type. Thus modeled high and low albedo fractions were input to the Equation (5).

As shown in Fig. 6, the range of urban impervious fraction was consistent with that of urban built area density in the mass. Several basic spatial patterns were found through further analysis. At first, urban impervious fraction was basically higher than 85% in the urban centre area between the east of People's Square, the west of Huangpu River and along the banks of the Suzhou River, where business centre and high density residential area were mainly distributed; then, urban

impervious fraction was between 60% and 85% in the area with industrial zones and moderate density residential area around the urban heartland; finally, urban impervious surface fraction basically varied from 20% to 60% in the outer region showing rapid urban sprawling.

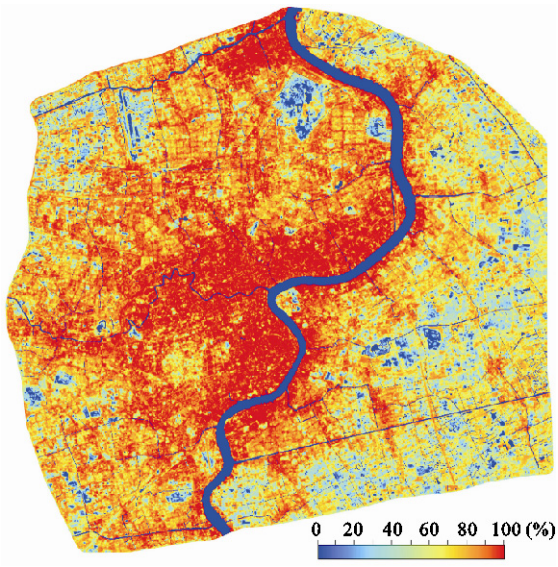


Fig. 6 Result of impervious surface estimation

### 3.3 Accuracy assessment and comparison

By digitized 'really' impervious surface value from aerial photograph an accuracy evaluation was performed. Figure 7 shows the comparison of the impervious surface estimating results and the residual between modeled fraction and actual fraction. It showed a much higher accuracy, except for several windows with the residual higher than 0.15, most samples were within ±0.1. According the Fig. 7, the number of overestimated samples was less than that of underestimated samples. But for the value of urban impervious surface fraction, there was overestimating trend as a whole.

Two types of error measurement, root mean square error (RMSE) and standard error (SE) were introduced to assess the accuracy of modeled impervious surface distribution. In order to show the estimation accuracy of improved method, a comparison with three researches was performed. Table 1 indicated that the improved method provided in this paper had a higher overall accuracy than traditional LSMA (obtaining impervious surface fraction by adding high and low albedo fractions directly) method applied by Yue and Wu (2007) and the normalized SMA (NSMA) model suggested by Wu (2004). Although with different samples, the result

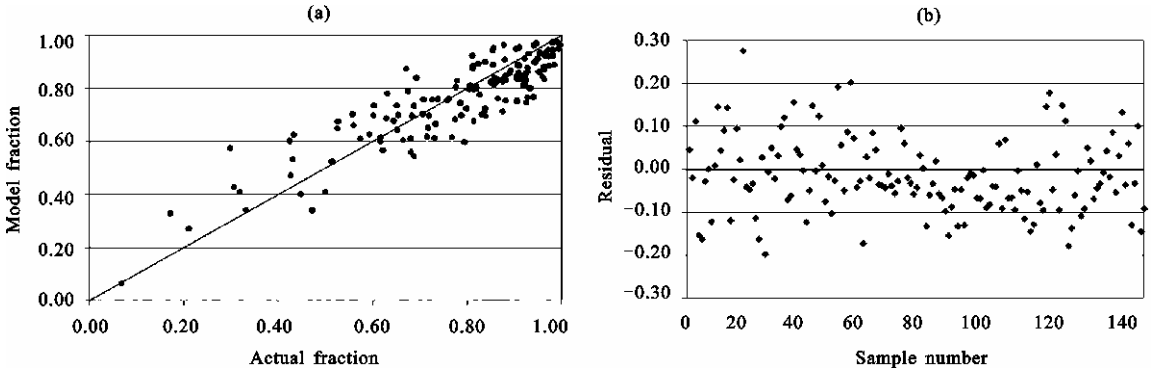


(a) Accuracy assessment of impervious surfaces estimation; (b) Residual analysis of impervious surface estimation

Fig. 7 Result of impervious surface estimation accuracy assessment

Table 1 Comparison of estimation accuracy with different methods

| Method | RMSE (%) | SE (%) | Sample number | Source |
|---|---|---|---|---|
| NSMA | 10.10 | –3.40 | 200 | Wu, 2004 |
| LSMA | 14.46 | –6.50 | 125 | Yue and Wu, 2007 |
| Improvement method | 8.01 | –1.23 | 145 | This paper |

still revealed that NSMA had a better accuracy than traditional LSMA, and obviously the improved method of this paper performed better than LSMA and NSMA with respect to RMSE and SE indices.

## 4 Discussion and Conclusions

### 4.1 Discussion

V-I-S composition, especially impervious surface fraction, has substantial potential for detecting and monitoring a wide variety of environmental change factors, including urban heat island, runoff, land use/cover change,

urban sprawl, population density, urban morphology, etc. There is a great need to estimate impervious surface distribution using mid-resolution remote sensing model for urban environment research, urban planning and urban management. The work performed by Ridd (1995), Small (2001; 2002; 2004), Wu and Murry (2003), Wu (2004), Weng et al. (2004), Weng and Lu (2008) and Lu and Weng (2005; 2006) has made a significant contribution to advancing the development and application of this model. However, there is still potential to explore the improvements in the estimation accuracy of impervious surfaces using remote sensing technology, as well as expansion of model application to different cities. Due to the high building density and extremely complicated spectral features of Shanghai, one of China's largest cities, it is necessary to determine representative urban spectrum composition by generalizing and grouping a number of land surfaces. Furthermore, a statistical method may produce more accurate impervious surface estimates, although the random sampling process is difficult and tedious. The role of shade provided by urban buildings and trees is a key factor in urban SMA modeling, even as a separated endmember in some researches. The effects of shade may vary from city to city. In the central area of Shanghai, there is very little shade from vegetation, but some vegetation in areas shaded by buildings was mistaken for low albedo, which resulted in a slight overestimation of impervious surface distribution. Further research is needed to eliminate this overestimation.

The application of mid-resolution remote sensing model to impervious surface estimation should be varied for different cities. For most Chinese cities with high building density, it is difficult to apply impervious surface estimation results to detailed urban regulatory planning, urban hydrological simulation, detailed population density estimates, and land use classification. However, the results can be used effectively for coarser scale applications, such as urban morphology, evaluation of urban biophysical and human systems, environmental management and urban master planning. In order to broaden the application of urban impervious surface estimation to more detailed scales, it is necessary to explore new estimation models based on remote sensing images at higher resolutions.

### 4.2 Conclusions

Through the estimation of the urban impervious surface distribution in the urban central area of Shanghai, it is indicated that it is possible to improve the urban impervious surface estimation accuracy for Chinese high density urban area based on mid-resolution Landsat images after a two-stage improvement. Urban average impervious surface fraction is more than 80% in Shanghai central area. The ratio is much higher than those of the comparative cities in most developed countries, so there is a big potential for Shanghai to improve its urban human settlement environment. In comparison with different research methods, this improved estimation method has a higher overall accuracy than traditional Linear Spectral Mixture Analysis (LSMA) method and the normalized SMA model both in root mean square error (RMSE) and standard error (SE). And the result of estimation could be applied to many urban planning and urban management fields. In the first stage improvement process, the key goal is just to improve selected endmembers quality, then get better endmember fraction; while in the second stage, it is to derive more accurate urban impervious surface really. So it is important to combine these two stages.

## Acknowledgements

The constructive suggestions and comments by anonymous reviewers and editors are greatly appreciated. Author also acknowledges Dresden for her dedication in English language and Yang for his dedication in drawing.

### References

Brabec E, Schulte S, Richards P L, 2002. Imperious surface and water quality: A review of current literature and its implications for watershed planning. *Journal of Planning Literature*, 16: 499–514.

Cai J, Victor F S, 2003. Measuring world city formation—The case of Shanghai. *The Annals of Regional Science*, 37: 435–446.

Deguchi C, Sugio S, 1994. Estimations for percentage of impervious area by the use of satellite remote sensing imagery. *Water Science Technology*, 29: 135–144.

Gilabert M A, Garcia-Haro F J, Melia J, 2000. A mixture modeling approach to estimate vegetation parameters for heterogeneous canopies in remote sensing. *Remote Sensing of Environment*, 72: 328–345.

Green A A, Berman M, Switzer P et al., 1988. A transformation for ordering multispectral data in terms of image quality with implications for noise removal. *IEEE Transactions on Geo-*

*science and Remote Sensing*, 26: 65–74.

Ji M, Jensen J R, 1999. Effectiveness of subpixel analysis in detecting and quantifying urban imperviousness from Landsat Thematic Mapper imagery. *Geocarto International*, 14(4): 31–39.

Lu D, Moran E, Batistella M, 2003. Linear mixture model applied to Amazonian vegetation classification. *Remote Sensing of Environment*, 87: 456–469. DOI: 10.1016/j.rse.2002.06.001

Lu D, Weng Q, 2005. Urban classification using full spectral information of Landsat ETM+ imagery. *Photogrammetric Engineering and Remote Sensing*, 71: 1275–1284.

Lu D, Weng Q, 2006. Use of impervious surface in urban land-use classification. *Remote Sensing of Environment*, 102: 146–160. DOI: 10.1016/j.rse.2006.02.010

Mustard J F, Sunshine J M, 1999. Spectral analysis for earth science investigations. In: *Manual of Remote Sensing, Volume 3*, *Remote Sensing for the Earth Sciences*. New York: John Wiley and Sons, Inc., 251–307.

Ridd M K, 1995. Exploring a V-I-S (vegetation-impervious surface-soil) model for urban ecosystem analysis through remote sensing: Comparative anatomy for cities. *International Journal of Remote Sensing*, 16: 2165–2185.

Slonecker E T, Jennings D, Garoflo D, 2001. Remote sensing of impervious surface: A review. *Remote Sensing Reviews*, 20: 227–255.

Small C, 2001. Estimation of urban vegetation abundance by spectral mixture analysis. *International Journal of Remote Sensing*, 22(7): 1305–1334.

Small C, 2002. Multitemporal analysis of urban reflectance. *Remote Sensing of Environment*, 81: 427–442.

Small C, 2004. The Landsat ETM+ spectral mixing space. *Remote Sensing of Environment*, 93: 1–17. DOI : 10.1016/j.rse.2004.06.007

Weng Q, Lu D, Schubring J, 2004. Estimation of land surface temperature-vegetation abundance relationship for urban heat island studies. *Remote Sensing of Environment*, 89: 467–483. DOI: 10.1016/j.rse.2003.11.005

Weng Q, Lu D, 2008. A sub-pixel analysis of urbanization effect on land surface temperature and its interplay with impervious surface and vegetation coverage in Indianapolis, United States. *International Journal of Applied Earth Observation*, (10): 68–83. DOI: 10.1016/j.jag.2007.05.002

Wu C, Murray A T, 2003. Estimating impervious surface distribution by spectral mixture analysis. *Remote Sensing of Environment*, 84: 493–505. DOI: 10.1016/S0034-4257(02)00136-0

Wu C, 2004. Normalized spectral mixture analysis for monitoring urban composition using ETM+ imagery. *Remote Sensing of Environment*, 93: 480–492. DOI: 10.1016/j.rse.2004.08.003

Xu Jianhua, Yue Wenze, Tan Wenqi, 2004. A Statistical study on spatial scaling effects of urban landscape pattern: A case study of the central area of the external circle highway in Shanghai. *Acta Geographica Sinica*, 59(6): 1058–1067. (in Chinese)

Yue W, Xu J, Wu J et al., 2006. Remote sensing of spatial patterns of urban renewal using linear spectral mixture analysis: A case of central urban area of Shanghai (1997–2000). *Chinese Science Bulletin*, 51(8): 977–986. DOI: 10.1007/s11434-006-097-7-8

Yue Wenze, Wu Cifang, 2007. Urban impervious surface distribution estimation by spectral mixture analysis. *Journal of Remote Sensing*, 11(6): 914–922. (in Chinese)